Journal of Applied Polymer Science

Efficient Benzodioxole-based unimolecular photoinitiators: From synthesis to photopolymerization under UV-A and visible LED light irradiation

Xiaoqing Dong,[1,2] Weizhen Shen,[1] Peng Hu,[1] Zhiquan Li,[1] Ren Liu,[1] Xiaoya Liu[1]

[1]The Key Laboratory of Food Colloids and Biotechnology, Ministry of Education, School of Chemical and Material Engineering, Jiangnan University, Wuxi, Jiangsu 214122, People's Republic of China

[2]Collaborative Innovation Center for Petrochemical New Materials, School of Chemistry and Chemical Engineering, Anqing Normal University, Anqing, Anhui 246013, People's Republic of China

Correspondence to: Z. Li (E-mail: lzq@jiangnan.edu.cn) and X. Liu (E-mail: lxy@jiangnan.edu.cn)

ABSTRACT: The narrow emission spectra of light emitting diodides (LED) as irradiation source has brought great challenge for the development of efficient photoinitiators sensitive to LED light. This paper described a series of novel unimolecular type II photoinitiators, containing thioxanthones as chromophores and benzodioxoles as coinitiators. The structures of the photoinitiators were characterized by ^{1}H NMR, ^{13}C NMR and high-resolution mass spectrometer. Study on the photophysical properties of the photoinitiators indicated that electron donors/acceptors as spacers between thioxanthone and benzodioxole affected both the UV–Vis absorption and the fluorescence emission. The long wavelength absorptions from 385 nm to 402 nm as well as low fluorescence quantum yields make the investigated benzodioxole derivatives quite attractive as efficient photoinitiators under UV-A and visible LED light irradiation. With a proper molecular design, the unimolecular photoinitiator exhibited higher initiation efficiency than the thioxanthone derivatives from the literature. Possible initiation mechanism was also proposed based on the photolysis study. © 2015 Wiley Periodicals, Inc. J. Appl. Polym. Sci. **2016**, *133*, 43239.

KEYWORDS: irradiation; photopolymerization; radical polymerization

Received 25 September 2015; accepted 22 November 2015
DOI: 10.1002/app.43239

INTRODUCTION

Photopolymerization technology has been widely used in various industrial applications including coatings, paints, inks, adhesives, optoelectronics, stereolithography, and nanotechnology.[1–3] The significant advantages such as spatial control, high productivity and low energy costs make photopolymerization superior to other polymerization methods.[4,5] However, traditional photopolymerization commonly employs medium or high pressure mercury lamps as irradiation sources with short UV light (UV-C and UV-B).[6–8] Excitation by short UV light suffers from some issues including production of ozone, radiation safety and limited curing depth. The inefficient mercury lamps are being substituted by some visible irradiation sources like the light emitting diode (LED) featuring irradiation safety and efficient energy utilization.[9–11]

In order to introduce LED light into photopolymerization applications, optimization of photoinitiating systems is needed so that the absorption of the photoinitiator/photosensitizer matches the emission of visible LED irradiation to ensure efficient photon absorption.[6,12] Unlike traditional mercury lamps with a broad emission spectra, the very narrow emission bandwidth of LED lamps at certain long wavelength (UV-A and visible light) has greatly limited the use of most commercial photoinitiators.[13] Among few examples suitably applied in LED photopolymerization, thioxanthones (TX) are quite attractive due to the long wavelength absorption between 360–420 nm and low fluorescence quantum yields,[14–16] which lead to a higher population of the triplet state preferable for the production of active radicals to initiate the polymerization.[17] Such well-known type II photoinitiators are generally used by combining with amines as efficient coinitiators. However, amines are apt to induce yellowing and toxicity.[18] Moreover, the intrinsic drawback of bimolecular system that the back electron transfer occurs between the excited TX and the amines, would decrease the initiation efficiency, especially in formulations of high viscosity.[19] Therefore, it is highly desirable to develop unimolecular thioxanthone-based photoinitiators without the above mentioned disadvantages.

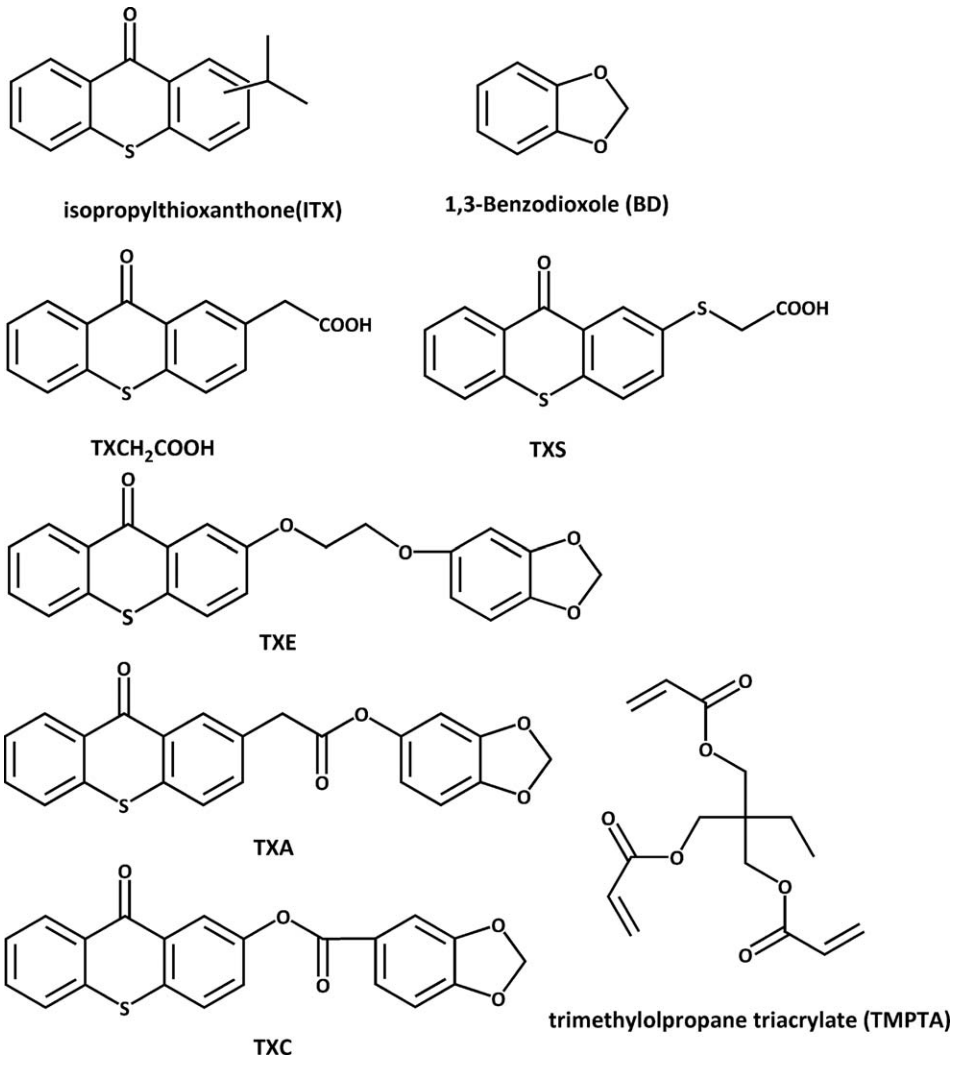

Figure 1. Structures of the investigated photoinitiators and the monomer.

Yagci *et al.* reported a series of thioxanthone acetic acid derivatives as efficient one component photoinitiators, which produced active free radicals via intramolecular hydrogen donating reaction followed by a rapid decarboxylation.[14,18] Altering the substitutions could extend the absorption up to 450 nm or even longer. On the other hand, Nie *et al.* demonstrated that as coinitiators, benzodioxole derivatives are good hydrogen donors with comparable reactivity of amines but much less yellowing and lower mammalian toxicity and antibacterial.[20–22] With a proper molecular design, such promising coinitiators should be chemically bound to thioxanthone to form one component photoinitiators sensitive to UV-A and visible light.

In this paper, a series of novel unimolecular photoinitiators containing TX as chromophores and benzodioxoles as coinitiators were synthesized (Figure 1). Spacers with different electron donating/accepting abilities enable the investigation of structure–property relationship. For comparison, the efficient photoinitiators thioxanthone acetic acid derivatives from the literature,[23–25] were also tested. Investigation on the photophysical properties of the photoinitiators was conducted via UV–Vis absorption and fluorescence emission. Photopolymerization kinetics and the properties of the cured films under UV-A and visible LED light irradiation were studied via real time FTIR (RT-FTIR) and pencil hardness tests, respectively. Possible initiation mechanism was proposed based on the electron spin resonance (ESR) study.

EXPERIMENTAL

Materials

Thiosalicylic acid and thiophenoxyacetic acid were purchased from Aladdin Industrial Corporation. Sesamol was obtained from J&K Scientific. Phenyl-N-tert-butyl-nitrone (PBN) was supplied by TCI Chemicals (Shanghai) Pvt. Dicyclohexylcarbodiimide, 4-dimethylaminopyridine, 1,3-benzodioxole and piperonylic acid came from Energy Chemical. Triphenylphosphine, phenol, sulfuric acid, thionyl chloride, 1,2-dibromoethane and the other solvents were bought from Sinopharm Chemical Reagent Co. The acrylate monomer trimethylolpropane triacrylate (TMPTA) was a gift from Jiangsu Sanmu Group. Column chromatography was performed with conventional techniques on

silica gel (200–300 mesh, Qingdao Haiyang Chemical Co.), and silica gel plates were used for TLC analyses. All the chemicals were used as received without further purification. Figure 1 lists the structures, abbreviations and their code names employed in this study.

Synthetic Procedures

Considering that the thioxanthone derivatives are photosensitive to visible light, the following preparation were performed in the dark.

Synthesis of Thioxanthone−Acetic Acid (TXCH$_2$COOH)

The synthesis of thioxanthone−acetic acid was well developed recently.[18,23,25] Thiosalicylic acid (1.54 g, 10mmol) was slowly added to 20 mL of concentrated sulfuric acid and the mixture was stirred for 30 min to ensure through mixing. Phenylacetic acid (4.05 g, 30 mmol) was added slowly to this stirred mixture. After the addition, this mixture was fiercely stirred for 2 hours at room temperature and then for 4 hours at 75°C. Then the mixture was cooled to room temperature and stirred overnight. Afterward, this mixture was slowly poured into boiling water (200 mL) with stirring, and precipitation was collected and washed with water to afford a crude blue solid, which was recrystallized from dioxane/water mixture to give the product as blue solid (1.97 g, yield: 68%). The product was directly used in the next step without further purification. ^{1}H NMR (400 MHz, DMSO) δ 12.53 (s, 1H), 8.52–8.34 (m, 2H), 7.92–7.49 (m, 5H), and 3.79 (s, 2H).

Synthesis of 2-Hydroxyl-Thioxanthone (TXOH)

Using a similar preparation manner to that of thioxanthone−carboxylic acid, 2-hydroxyl- thioxanthone was obtained as an orange powder (yield: 38%). ^{1}H NMR (400 MHz, DMSO) δ 10.18 (s, 1H), 8.46 (m, 1H), 7.90–7.52 (m, 5H), 7.32–7.23 (m, 1H).

Synthesis of 2-Thioxanthone-Thioacetic Acid (TXS)

Using a similar preparation manner to that of thioxanthone−carboxylic acid, 2-thioxanthone-thioacetic acid was obtained as an orange powder by replacing thioxanthone−carboxylic acid with thiophenoxyacetic acid (yield: 35%). ^{1}H NMR (400 MHz, DMSO) δ 12.78 (s, 1H), 8.48–7.55 (m, 7H), 3.97 (s, 2H).

Synthesis of 5-(2-bromo-ethoxy)-Benzo[1,3]Dioxole (BrBD)

A mixture of sesamol (1.38 g, 0.01 mol), sodium hydroxide (0.8 g, 0.02 mol) and water (30 mL) were stirred together for half an hour at room temperature. And dropwised a solution of tetrabutyl ammonium bromide (0.35 g, 1.5 mmol) in 30 mL 1,2-dibromoethane. The solution was refluxed overnight. After cooled to room temperature, the mixture was washed with water and dried overnight by anhydrous sodium sulfate. A brown solid was obtained by rotary evaporator and further purified by column chromatography with dichloromethane as eluent to afford colorless solid (1.1 g, yield: 56%). ^{1}H NMR (400 MHz, $CDCl_3$) δ 6.81–6.28 (m, 4H), 5.95 (s, 2H), 4.24 (*t*, $J = 6.3$ Hz, 2H), 3.62 (*t*, $J = 6.3$ Hz, 2H).

Synthesis of Benzo[1,3]dioxole-5-Carbonyl Chloride (PACl)

A mixture of 2.52 g (18 mmol) of piperonylic acid, 2.2 g (38 mmol) of thionyl chloride, 3 drops of DMF, and 80 mL of dry anhydrous chloroform was put into a round-bottomed flask and heated to reflux until the mixture was clear. A white solid piperonyloyl chloride was obtained after removing the solvent under vacuum (2.76 g, yield: 82%).

Synthesis of (9-oxo-9H-thioxanthen-2-yl)-Acetic Acid Benzo[1,3]Dioxol-5-Yl Ester (TXA)

A mixture of sesamol (0.138 g, 1 mmol), thioxanthone−carboxylic acid (0.27 g, 1 mmol), dicyclohexylcarbodiimide (DCC, 0.78 g, 3.5mmol), 4-dimethylaminopyridine (DMAP, 0.12 g, 1 mmol) and dry dichloromethane (50 mL) were stirred together for 1 h in a flask equipped with stirrer at room temperature for 24 hours. Thin-layer chromatography was used to identify the process of reaction. After the sesamol was completely consumed, the solution was washed with water (3 × 50 mL) and dried overnight by anhydrous sodium sulfate, then evaporated under reduced pressure to afford crude product, which was further purified by column chromatography with dichloromethane as eluent to afford orange solid (0.144 g, yield: 36%). ^{1}H NMR (400 MHz, $CDCl_3$) δ 8.68–8.60 (m, 2H), 7.74–7.49 (m, 6H), 6.79–6.53 (m, 3H), 5.99 (s, 2H), 3.99 (s,2H). ^{13}C NMR (101 MHz, $CDCl_3$) δ 137.18, 136.34, 133.37, 132.37, 131.83, 130.50, 129.94, 129.15, 126.54, 126.42, 126.06, 113.80, 107.96, 103.57, 101.72, 77.69, 77.22, 76.41, 55.70, 40.84, 30.93. Q-Tof-MS (m/z): calcd for $C_{22}H_{15}O_5S$, 391.0640. Found: 391.0601 $[M+H]^+$

Synthesis of 2-[2-(benzo[1,3]dioxol-5-yloxy)-ethoxy]-Thioxanthen-9-One (TXE)

Anhydrous potassium carbonate (0.548 g, 30 mmol) was added to the solution of 2-hydroxyl-thioxanthone (0.231 g, 1 mmol) in 12 mL of acetonitrile at room temperature under a nitrogen atmosphere. The mixture was stirred vigorously for 2 hours. 0.242 g (1 mmol) of 5-(2-bromo-ethoxy) benzodioxole dissolved in 10 mL of acetonitrile was slowly added, then the mixture was allowed to reflux for 24 hours. After the reaction the mixture was cooled to room temperature. The precipitate was filtered off and washed three times with 10 mL acetonitrile. The organic layers were combined and the solvent was removed under vacuum to afford an orange solid. The crude product was further purified by column chromatography with dichloromethane as eluent to afford TXE as orange solid (0.18 g, yield: 23%). ^{1}H NMR (400 MHz, $CDCl_3$) δ 8.70–8.64 (m, 1H), 8.15 (d, $J = 2.9$ Hz, 1H), 7.68–7.49 (m, 4H), 7.36 (m, 1H), 6.75 (d, $J = 8.5$ Hz, 1H), 6.60 (d, $J = 2.5$ Hz, 1H), 6.42 (m, 1H), 5.95 (s, 2H), 4.47 (m, 2H), 4.34 (m, 2H). ^{13}C NMR (101 MHz, $CDCl_3$) δ 179.64, 157.46, 154.06, 148.31, 142.07, 137.51, 132.08, 130.24, 129.91, 128.63, 127.43, 126.14, 126.02, 123.25, 111.23, 107.95, 106.08, 101.20, 98.55, 77.21, 67.51, 67.01. Q-Tof-MS (m/z): calcd for $C_{22}H_{17}O_5S$, 393.0797. Found: 393.0776 $[M+H]^+$.

Synthesis of Compound Benzo[1,3]dioxole-5-Carboxylic Acid 9-oxo-9H-Thioxanthen-2-Yl Ester (TXC)

0.185 g (1 mmol) of piperonyloyl chloride was reacted with 2-hydroxyl- thioxanthone (0.23 g, 1 mmol) and triethylamine (0.5 mL, 3.5 mmol) in 10 mL of anhydrous chloroform at room temperature for 6 hours. The mixture was washed twice with 15 mL 1*M* $NaHCO_3$ and 15 mL of water, and the organic phase was dried overnight with anhydrous sodium sulfate. This

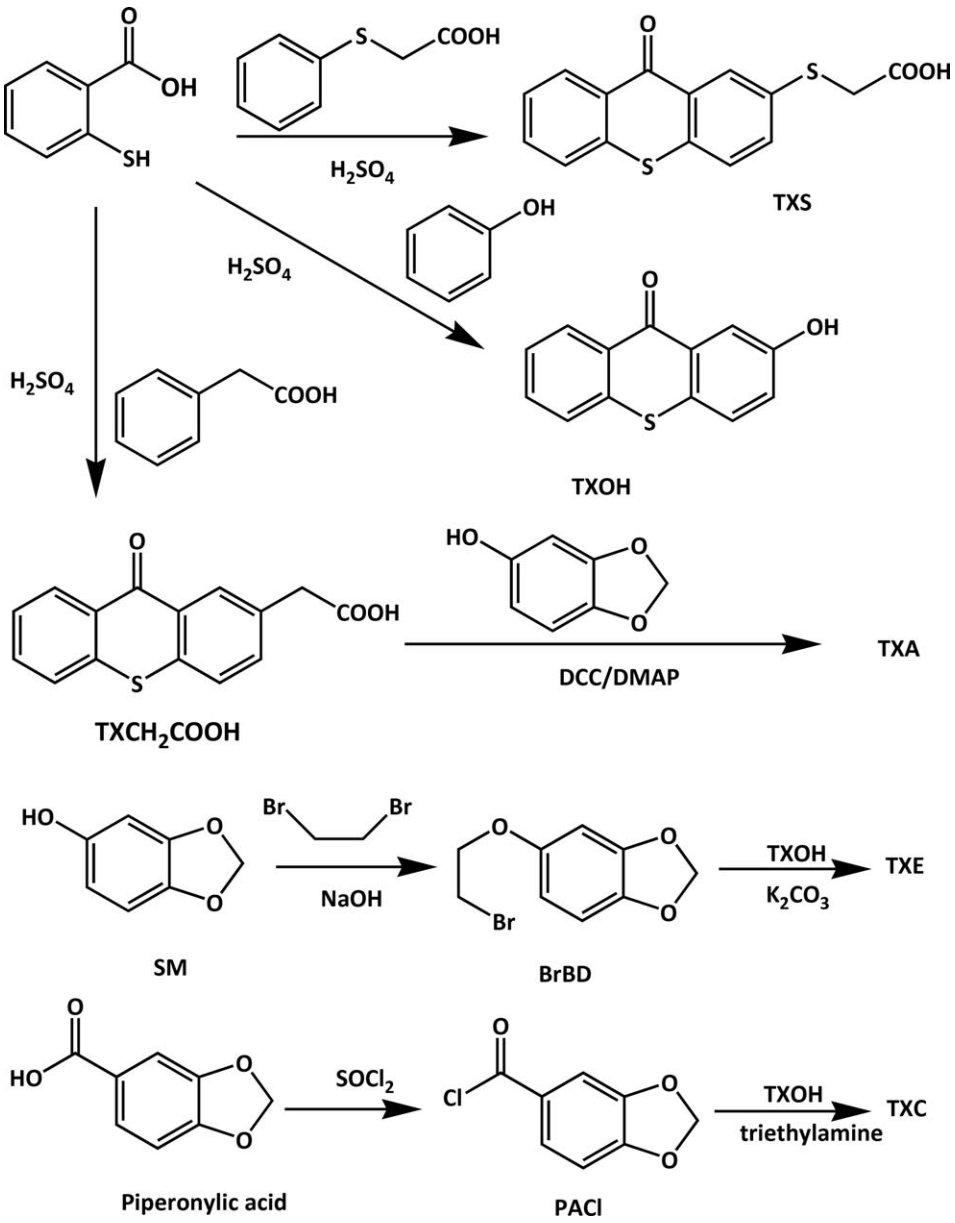

Scheme 1. Synthetic routes of the novel photoinitiators.

organic phase was concentrated and purified by column chromatography with dichloromethane as eluent to obtain light orange solid. (0.166 g, yield: 44%). ^{1}H NMR (400 MHz, $CDCl_3$) δ 8.64–8.60 (m, 1H), 8.42 (d, $J = 2.5$ Hz, 1H), 7.85 (m, 1H), 7.64–7.49 (m, 7H), 6.92 (d, $J = 8.2$ Hz, 1H), 6.09 (s, 2H). ^{13}C NMR (101 MHz, $CDCl_3$) δ 178.30, 163.34, 151.46, 148.43, 147.00, 136.13, 133.38, 131.42, 129.33, 128.94, 127.62, 126.22, 125.95, 125.47, 125.43, 125.03, 121.86, 121.23, 108.97, 107.25, 101.04. Q-Tof-MS (m/z): calcd for $C_{21}H_{13}O_5S$, 377.0484. Found: 377.0307 $[M+H]^+$.

Characterization

^{1}H NMR and ^{13}C spectrum were measured using a Bruker instrument (AVANCE III HD 400 MHz). UV-Vis spectra were measured with a Beijing Purkinje TU-1901 UV-VIS spectrophotometer. The incident light intensity was monitored by radiometers (UV-A, Photoelectric Instrument Factory of Beijing Normal University; UV-int140 from DESIGN Germany). The UV Pro YW-51220 LED lamp irradiated 365 nm and 405 nm light came from Shanghai UV Pro Co. The polymerization experiments were carried out using real-time FTIR with a Nicolet 6700 FT-IR spectrometer worked with an OmnicCure Series 1000 UV spot curing system, which was adjusted the incident light intensity according to the monitor of UV-Integrator 140 power meter or radiometers. The hardness of coatings was evaluated by BY Pencil hardness tester purchased from Shanghai Pushen Chemical machinery Co. ESR spin-trapping spectrum was measured in benzene using a Bruker EMXplus-10/12. The fluorescence intensities and fluorescence quantum yields were recorded on a Varian Cary Eclipse Fluorescence

Spectrophotometer. The fluorescence intensities and fluorescence quantum yields were estimated by using quinine sulfate in 0.1*M* H_2SO_4 as the standard and using the following equation[26]:

$$\text{Fluorescence quantum yields } (\varphi_f) = \varphi_{st} \times I_f/I_{st} \times \eta_f/\eta_{st}^2 \times A_{st}/A_f$$

where φ_f stands for the fluorescence quantum yield of the sample (*f*) and standard (*st*), *A* is the absorbance at the excitation wavelength, *I* denotes the relative intensity of the exciting light and η is the average refractive index of the solution.

Electron Spin Resonance Spin-Trapping

The ESR experiments were carried out using an EMXplus-10/12 X-band spectrometer at 100 kHz magnetic field modulation, which was used to adjust the power intensity to 20 mW. The mixture of photoinitiators (1 mol %) and Phenyl-N-tert-butylnitrone (PBN, 2 mol %) was dissolved in benzene and deoxygenated with nitrogen for 5 min before irradiation.[22,27–29] The radicals were generated through photolysis at room temperature (LED source emitting 365 nm light, irritation for 60 s).

Real-Time FTIR

Real-time FTIR spectroscopy was used to monitor the double band conversion as a function of exposure of irradiation in the resins. An Hg lamp adapted to the FTIR spectrometer by means of a light guide was used to adjust the light intensity to 24.5 mW/cm^2 and to irradiate the resins. Photoinitiators and triphenylphosphine (2 mol %) were dissolved in 0.3 mL dichloromethane, which were added to the corresponding monomers and well-mixed by ultrasonic vibration for 10 minutes. Before the photopolymerization, the mixture was dried under vacuum for 30 minutes at room temperature in order to remove the solvent. The thickness of the mixture film was adjusted by a 120 μm film applicator (BYK). Polymerization profiles were recorded during 300 s irradiation at room temperature. For each sample, the real-time FTIR runs were repeated three times. The polymerization kinetics were measured by monitoring the disappearance of double band and the double bond conversion was calculated using the formula[30]:

$$\text{Double band Conversion (DC, \%)} = [1 - A_t/A_0] \times 100\%$$

where A_t is the area of the double band characteristic absorbance peak at 810 cm^{-1} at time *t*,[31] and A_0 stands for the initial area of this peak.

Photopolymerization and Pencil Hardness Test

The above mentioned mixtures were coated on glass plates and adjusted the thickness of the film by the 120 μm film applicator. Curing was carried out using YW-512020 UV PRO equipped with a LED light source emitting light at 365 nm and 405 nm. The conveyor belt of the curing system was set at 5 m/min. The coated glass plates were placed on the conveyor of the YW-512020 UV PRO curing system and passed under the irradiation source. The hardening and eventual full curing of the films were measured by pencil hardness. The results recorded were the number of passes under each irradiation source to give a fully cured film,[32] which were determined by pencil hardness (6H).

The pencil hardness of the irradiated films was evaluated by scratching the coatings with pencils according to GB/T 6739-1996, which was a simple method to test the scratch hardness by moving pencils with different hardness scratched over the coating film with a given angle and constant pressure.

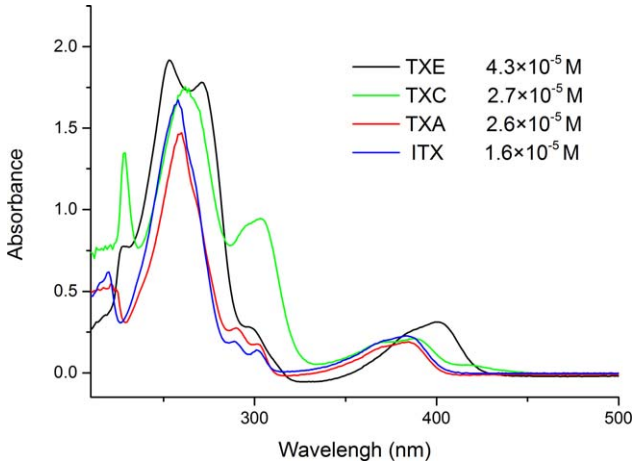

Figure 2. Absorption spectra of photoinitiators in acetonitrile solution. [Color figure can be viewed in the online issue, which is available at wileyonlinelibrary.com.]

RESULTS AND DISCUSSION

Synthesis of Benzodioxole-Based Unimolecular Photoinitiators

Benzodioxole is chosen to play the role of a coinitiator because benzodioxole derivatives are good hydrogen donors with much less yellowing and lower mammalian toxicity compared to amines.[33,34] In order to study the structure–property relationship, benzodioxole moiety was introduced into the thioxanthone backbone with different spacers. Photoinitiators TXA and TXC comprise ester groups as spacers with electron-drawn ability, while TXE contains ethylene glycol with electron-donating ability. The photoinitiators were prepared as described in Scheme 1.

For the preparation of TXA and TXC, the important thioxanthone precursors with acetic acid (or hydroxy) moiety were synthesized via cyclization between thiosalicylic acid and phenylacetic acid (or phenol) in the presence of concentrated sulfuric acid. Subsequent esterification reactions were carried out using two methods. For TXA, the esterification of thioxanthone acetic acid and sesamol was performed catalyzed by DCC/DMAP, while the synthesis of TXC included the esterification of hydroxyl-thioxanthone and piperonyloyl chloride. Both methods are efficient to produce ester groups as spacers to link the benzodioxole moiety and the TX backbone. The synthesis of TXE containing an electron donating spacer ethylene glycol was performed via Williamson reactions between hydroxyl-thioxanthone and the corresponding bromide precursor.

For comparison, 2-thioxanthone-thioacetic acid (TXS) and 2-thioxanthone-acetic acid ($TXCH_2COOH$), two highly efficient unimolecular Type II photoinitiators in literature[23–25] based on photodecarboxylation mechanism, were also synthesized according to Yagci *et al.* without modification.[18]

Table I. Photophysical Properties of the Photoinitiators[a]

	λ_{max} (nm)	ε_{365}	ε_{405}	ε_{max}	λ_{ex} (nm)	λ_{em} (nm)	Fluorescence quantum yields (φ_f,%)
TXE	402	2233	6813	7720	392	439	9.44×10^{-2}
TXC	388	6592	2777	8037	408	460	2.95×10^{-2}
TXA	385	6153	1038	8308	383	416	1.16×10^{-2}
ITX	387	4045	1181	6500	381	414	3.04×10^{-2}
TXS[25]	384			3900	384	438	6×10^{-2}
$TXCH_2COOH$[23]	385	3547	1621	5500	380	409	9×10^{-2}

[a] Where ε_{365}, ε_{405}, and ε_{max} (L mol^{-1} cm^{-1}) stand for the molar extinction coefficient at 365 nm, 405 nm and λ_{max}, respectively. λ_{ex} and λ_{em} are the maximum fluorescence excitation and emission of photoinitiators in acetonitrile solution (10^{-5} *M*). Fluorescence quantum yields measurements in acetonitrile using quinine sulfate as a standard.

Photophysical Properties

Figure 2 depicted the UV–Vis absorption spectra of the novel photoinitiators in acetonitrile at room temperature. All of them exhibited broad absorption band with the position of the maximum ranging from 385 up to 402 nm. The absorption peaks of TXA at 278 nm and 385 nm are attributed to the π-π^* transition and n-π^* transition, respectively.[35] Since the introduction of the ethoxycarbonyl group did not significantly change the electronic structure of the thioxanthone chromophore, the shape and the wavelength of the absorption peaks of TXA were quite similar to thioxanthone.

When substituting the spacer from ethoxycarbonyl to ethylene glycol as in TXE, the maximum absorption red-shifted nearly 20 nm up to 402 nm. The enhancement was attributed to the increased electron donating ability of the oxygen. The electronic effect on absorption of the chromophore can be confirmed when investing TXC with methyl ester as the spacer. The electron drawing property of the methyl ester directly attach to the thioxanthone moiety induced a blue-shift of the maximum absorption of TXC down to 388 nm. In a word, the long wavelength absorption ranging from 385 up to 402 nm makes the novel photoinitiators sensitive to UV-A and visible light.

Unlike traditional mercury lamps with a broad emission spectra, the very narrow emission bandwidth of LED lamps at certain long wavelength brings great challenge to match the absorption of the photoinitiators to the emission of the LED lamps. Since 365 nm and 405 nm LED light were used for the subsequent photopolymerization tests, more attention should be paid to the absorption at these two wavelengths. As shown in Table I, TXA and TXC with electron drawing spacers exhibited larger extinction coefficients at 365 nm but much weaker absorption at 405 nm compared to TXE with an electron donating spacer. The tunable photosensitivities make the photoinitiators more flexible for the specific applications.

UV–Vis spectra can only provide the information of photon-absorption behavior of the photoinitiators. Strong absorption is not necessarily an indication of an efficient initiation because the absorbed energy can induce other deactivation processes such as fluorescence and thermal conversion. Therefore, low fluorescence quantum yields are preferred for an efficient Type II photoinitiator as this leads to a higher population of the triplet state, which is the active state of the initiator reacting with a hydrogen donor to produce active free radicals for the subsequent polymerization.[35]

The fluorescence spectra and fluorescence quantum yields (φ_f) of the photoinitiators were investigated in acetonitrile at room temperature using quinine sulfate (in 0.1*M* H_2SO_4, $\varphi_f = 54\%$) as a standard with an excitation wavelength of 360 nm.[36] As shown in Table I, the fluorescence quantum yields of the commercial initiator isopropylthioxanthone (ITX) is 3.04×10^{-2}. The very low φ_f of ITX ensure high quantum yields of inter system crossing (ISC). The efficient ISC combined with long triplet lifetime makes thioxanthone attractive as Type II photoinitiator.[23] Thioxanthone derivative with an electron drawing spacer as in TXC exhibited nearly identical φ_f to ITX, with the value of 2.95×10^{-2}. Reduction to nearly 1/3 was found for the φ_f of TXA. When replacing the electron drawing spacer by the electron donating one as in TXE, the φ_f increased up to three times compared to that of ITX. The introduction of electron donating substitution not only induced red-shift in absorption, which is favorable for LED irradiation with long wavelength, but also results in the enhancement of fluorescence, which is detrimental for the generation of active free radicals to initiate the polymerization.

Photolysis Study

Beside UV–Vis absorption and fluorescence emission tests, steady-state photolysis experiments can also provide useful information to study the photo behavior of the photoinitiators. The steady-state photolysis tests were performed in acetonitrile at room temperature under irradiation with different light doses. Changes in the shape and the intensity of the absorption bands indicated the occurrence of the photoinduced decomposition (Figure 3). The absorption peaks of TXA at 260 nm and 384 nm decreased with the increased light doses. In the mean time, a new peak appeared at 318 nm with increased intensity. It should be mentioned that the decreased absorption at 384 nm is beneficial for deep photocuring because the photolysis products do not absorb the LED irradiation light (365 nm and 405 nm), allowing the light to penetrate deeper into the resin to realize depth polymerization.

The same trend was also observed for another two photoinitiators TXC and TXE. The changes of the UV–Vis absorption

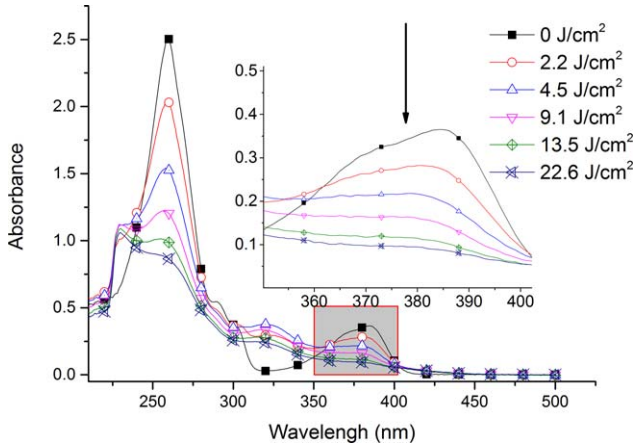

Figure 3. Photolysis of TXA solution ($4.0*10^{-5}$ *M*) irradiated with different light doses. [Color figure can be viewed in the online issue, which is available at wileyonlinelibrary.com.]

might be attributed to the photo-decomposition of TXA, which included the hydrogen abstraction between the excited thioxanthone and the benzodioxole moiety via inter- or intramolecular reaction, forming ketyl radicals and cyclic acetal radicals.[37]

In order to confirm the generation of the radicals after photolysis, ESR measurements were carried out using PBN as spin trap and benzene as solvent.[38] ESR spectrum of TXA after irradiation was shown in Figure 4. The ESR signal demonstrated the generation of the free radicals. Only one spin trap product was observed with the hyperfine splitting constants (HFS) for nitrogen (a_N) and hydrogen (a_H) with the values of 14.4 G and 2.3 G, respectively. The signal should be derived from the formed cyclic acetal radicals rather than the ketyl radicals because the latter radicals are highly stable,[39] which could not be trapped by PBN.[27] Similar results of trapping the generated cyclic acetal radicals were reported by Nie *et al.*[22]

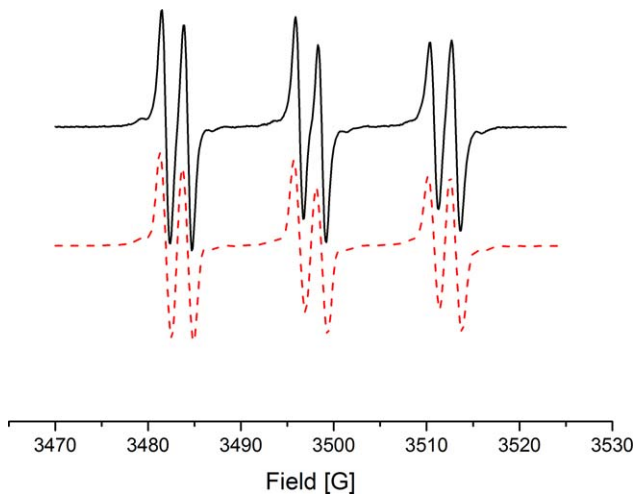

Figure 4. ESR spectra of TXA with PBN in benzene under 365 nm LED light: (up) experimental spectra and (down) simulated spectra. [Color figure can be viewed in the online issue, which is available at wileyonlinelibrary.com.]

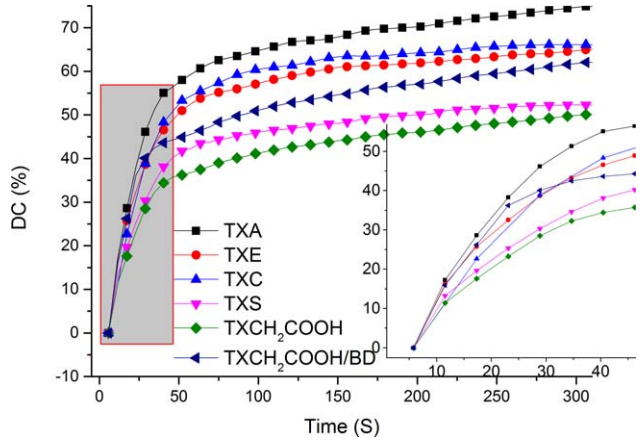

Figure 5. Double bond conversion of resins with different photoinitiators (1 mol %) in the presence of TPP (2 mol %), irradiated by an Hg lamp with an intensity of 40 mW/cm^2. [Color figure can be viewed in the online issue, which is available at wileyonlinelibrary.com.]

Photopolymerization

The initiating efficiency of the photoinitiators irritated under UV-A and visible light was evaluated via the photoinduced crosslinking reaction of the acrylate monomers. The formulations for the photopolymerization tests contained trifunctionality acrylate monomer TMPTA and the investigated photoinitiators with different concentrations. Although the one-component photoinitiators possess similar chemical structures with a thioxanthone backbone and a benzodioxole moiety, the solubility of the photoinitiators in the formulation was affected by the type of the spacers following the order: TXA > TXC > TXE. The favorable solubility of TXA containing the electron-drawn spacer might be attributed to the electronic effect between this spacer and thioxanthone backbone.[23] Good solubility is preferred as it generally provides better compatibility of formulation to ensure enhanced photopolymerization performance. Moreover, improved solubility of the photoinitiator provides possibility to prepare the formulation with higher concentration required for some specific applications. In order to reduce oxygen inhibition, 2 mol % of triphenyl phosphine (TPP) was added as an anti-oxygen inhibition additive.[40,41]

To examine the kinetic of photopolymerization, we monitored the conversion during irradiation employing real-time Fourier transform infrared (FT-IR) spectroscopy. Photopolymerization profiles were recorded during 300 s irradiation at room temperature using an OmnicCure Series 1000 UV spot curing system. The conversion was recorded by monitoring the disappearance of the double bond at 810 cm^{-1} (Figure 5). All the investigated photoinitiators could induce the polymerization of TMPTA under irradiation. The polymerization proceeded rapidly at the beginning of the irradiation due to the fast consumption of the photoinitiators and then slowly down after 50 s. $TXCH_2COOH$ and TXS are two efficient one component photoinitiators in literature.[23–25] The initiation mechanism involves intramolecular electron transfer followed by hydrogen abstraction. After a rapid decarboxylation, active free radicals are formed to induce the polymerization.[25] The initiation process did not require additive H-donor as coinitiators. Both photoinitiators could induce the

Table II. Conversion after 300 s with Different Photoinitiator Concentrations

Concentration of photoinitiator (mol %)	TXA	TXE	TXC	TXS	$TXCH_2COOH$	$TXCH_2COOH$/BD
0.5	70 ± 6	58 ± 9	57 ± 7	50 ± 4	47 ± 5	57 ± 4
1.0	73 ± 4	61 ± 7	62 ± 4	52 ± 5	50 ± 5	62 ± 6
2.0	74 ± 4	65 ± 9	70 ± 7	56 ± 4	58 ± 7	65 ± 7

photopolymerization with the double bonds conversion of around 50%.

Adding benzodioxole as a coinitiator into the formulation containing $TXCH_2COOH$ resulted in the improved conversion up to about 62%. The result suggested that benzodioxole was an efficient coinitiator. The physical mixture of the photoinitiator and the coinitiator might suffer from the intrinsic drawback of the bimolecular initiating system, such as diffusion controlled limitation and deactivation from back electron transfer.[42] Therefore, higher efficiency is expected for the unimolecular photoinitiator. For TXA with the coinitiator benzodioxole chemically attached to thioxanone, improved conversion up to about 73% was obtained. Although both TXC and TXA contain ester group as the spacer, TXC exhibited slower curing rate and lower conversion than TXA. The enhancement of TXA might be attributed to the lower quantum yields of fluorescence, which were preferred to induce a higher population of the triplet state and therefore beneficial for the generation of active free radicals.

The electronic density of benzodioxole derivatives has significant effect on the activity of the formed benzodioxole free radicals.[20] Generally, an electron-donating group on the benzene ring can increase the initiation efficiency because of the suppression of the aromatic effect. Inefficient aromatic effect would decrease the extended electronic delocalization of the lone electron pairs of the oxygen atoms and therefore ensure higher electronic density available to participate in the initiation process. On the other hand, the electron-withdrawing substituents induce lower electronic density of the benzodioxole free radicals, leading to lower initiation efficiency.[43,44] Therefore, TXE containing ethylene glycol as the spacer should exhibit superior performance to TXA and TXC with electron-drawn spacers. However, TXE displayed only comparable conversion to TXC, lower than TXA. The inferior performance of TXE may be attributed to its much higher quantum yields of fluorescence compared to TXA and TXC. Strong fluorescence is unfavorable for the higher population of the triplet state and thus for the generation of active free radicals.

Effect of the photoinitiator concentration on the double bond conversion was shown in Table II. Among the investigated photoinitiators (or photoinitiating system), increased concentration of the photoinitiator from 0.5 mol % to 2 mol % resulted in higher conversion. It should be noted that higher concentration of the photoinitiator was not always favorable because in the fast photopolymerization reactions, taking UV curing for coating applications as an example, only less than 10–15% of the initiators are consumed during the light irradiation. Higher concentration means more photoinitiators left after curing. The residual photoinitiators are apt to migrate through the cured coatings and affect the properties of the formed films. Moreover, unsuitably higher concentration of the photoinitiator is prone to induce inner filter effects, which can decrease the penetration of the light and lead to less amount of photons absorbed by the initiators.

Photopolymerization tests were also performed under UV-A (365 nm) and visible (405 nm) LED light irradiation. The same formulation used in RT FTIR tests were coated on the glass plates to give 120 μm thick film and then placed on the conveyor of the YW-512020 UV PRO curing system, passing through under the LED light exposure. The number of passes were recorded until a fully cured film was obtained (Table III).

For 365 nm LED irradiation, TXA, with suitable absorption as well as low fluorescence emission, exhibited the highest curing speed with only two passes to obtain a full cured film. More passes were needed for TXE than for TXC. The slower curing speed of TXE with the electron donating spacer might be explained by the red-shift absorption (402 nm) and relatively stronger fluorescence. Although the absorption of TXE (402 nm) well matches the visible LED light of 406 nm, the curing speed of TXE was still slower than that of TXA under visible LED irradiation. The result indicated that for the initiation efficiency of these two photoinitiators, the quantum yields of the free radicals played a more important role than the light absorption and the initiation ability of the radicals. Due to the inefficient absorption at the long wavelength, TXC required more passes than TXE.

For both 365 nm and 405 nm LED irradiation, the curing speed of the unimolecular benzodioxole photoinitiators were faster than the bimolecular system. Moreover, less passes were needed

Table III. Curing Results Quoted the Number of Passes to Obtained a Fully Cured Film under the 365 and 405 nm LED Lamp[a]

	Passes to full cure	
Photoinitiators	LED source (365 nm)	LED source (405 nm)
TXA	2	6
TXE	5	7
TXC	4	10
TXS	7	11
$TXCH_2COOH$	7	14
$TXCH_2COOH$ +BD	6	9

[a] Fully cured films were determined by pencil hardness (6H).

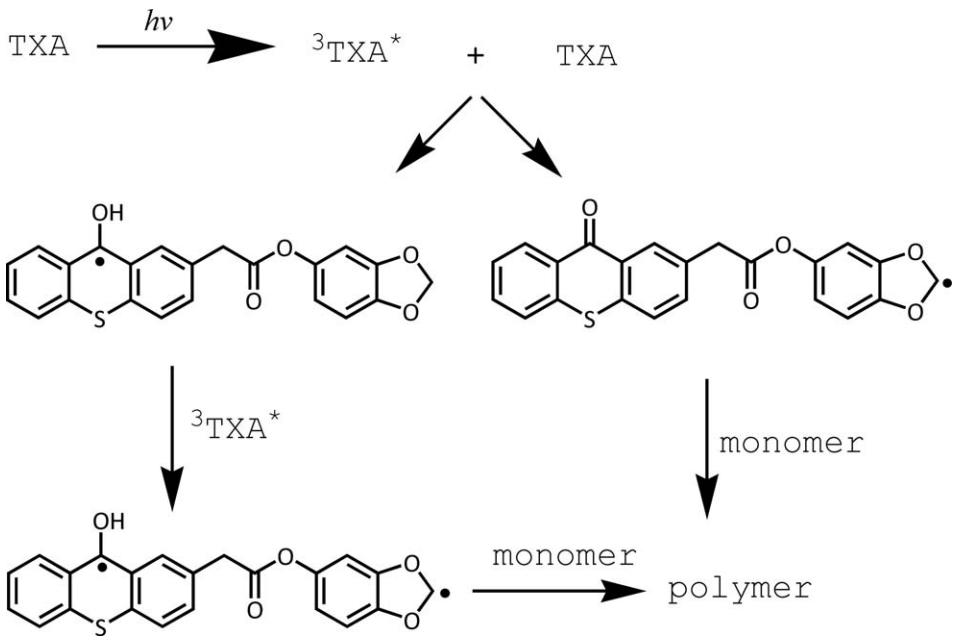

Scheme 2. Proposed polymerization mechanism of TXA.

for the novel benzodioxole-based photoinitiators than for the two reference photoinitiators (TXS and $TXCH_2COOH$) due to the highly efficient initiation ability of the benzodioxole radicals.

On the basis of the photolysis results and the photopolymerization behavior combined with previous study on the thioxanthone derivatives,[23,45] the polymerization mechanism of the benzodioxole-based photoinitiators was proposed (Scheme 2). The parent thioxanthone works as a photosensitizer to absorb the UV-A and visible light. Via intra- and inter-molecular reaction, hydrogen transfers from the the benzodioxole group to the excited thioxanthone. The formed ketyl radicals cannot initiate the polymerization because of sterical hindrance and delocalization of an unpaired electron.[37] While the generated cyclic acetal radicals can efficiently initiate the polymerization.

CONCLUSIONS

In conclusion, a series of novel unimolecular photoinitiators containing thioxanthone as chromophores and benzodioxole as coinitiators were successfully prepared. Investigation on the photophysical properties of the photoinitiators indicated that electron donors/acceptors as spacers between thioxanthone and benzodioxole affected both the UV–Vis absorption and the fluorescence emission. The introduction of the spacer with electron donating property induced red-shift in absorption, which was favorable for LED irradiation with long wavelength as well as stronger fluorescence. Fluorescence is detrimental for the generation of active free radicals to initiate the polymerization. In photopolymerization tests, all the novel photoinitiators could induce the polymerization of TMPTA under 365 and 405 nm light. Among the investigated photoinitiators, TXA, with suitable absorption as well as low fluorescence emission, exhibited the best performance with the highest double bond conversion and the fastest curing rate. The curing speed of the unimolecular benzodioxole photoinitiators were faster than the bimolecular initiating system. Moreover, due to the highly efficient initiation ability of the benzodioxole radicals, the novel benzodioxole-based photoinitiators exhibited faster photopolymerization rate and higher double bond conversion than the two reference unimolecular photoinitiators. Possible initiation mechanism was proposed including hydrogen transfers from the benzodioxole group to the excited thioxanthone, forming active cyclic acetal radicals to initiate the polymerization.

ACKNOWLEDGMENTS

The authors thank the National Nature Science Foundation of China (21404048 and 21307002) and the Fundamental Research Funds for the Central Universities (JUSRP 11513 and 51507) for financial support.

REFERENCES

1. Keitz, B. K.; Yu, C. J.; Long, J. R.; Ameloot, R. *Angew. Chem. Int. Ed.* **2014**, *53*, 5561.
2. Crivello, J. V.; Reichmanis, E. *Chem. Mater.* **2014**, *26*, 533.
3. Lalevee, J.; Blanchard, N.; Tehfe, M.; Peter, M.; Morlet-Savary, F.; Gigmes, D.; Fouassier, J. P. *Polym. Chem.* **2011**, *2*, 1986.
4. Crivello, J. V.; Dietliker, K. Photoinitiators for Free Radical Cationic & Anionic Photopolymerisation; Wiley: Weinheim, **1999**.
5. Chatani, S.; Kloxin, C. J.; Bowman, C. N. *Polym. Chem.* **2014**, *5*, 2187.
6. Xiao, P.; Zhang, J.; Dumur, F.; Tehfe, M. A.; Morlet-Savary, F.; Graff, B.; Gigmes, D.; Fouassier, J. P.; Lalevée, J. *Prog. Polym. Sci.* **2015**, *41*, 32.
7. Yagci, Y.; Jockusch, S.; Turro, N. J. *Macromolecules* **2010**, *43*, 6245.
8. Nan, X.; Huang, Y.; Fan, Q.; Shao, J. *J. Appl. Polym. Sci.* **2015**, *132*, 42361.

9. Shi, S.; Allonas, X.; Croutxé-Barghorn, C.; Chemtob, A. *New J. Chem.* **2015**, *39*, 5686.
10. Kiyoi, E. *Eur. Coat. J.* **2013**, *10*, 26.
11. Kim, S.; Cho, J. K.; Shin, S.; Kim, B. *J. Appl. Polym. Sci.* **2015**, *132*, 42726.
12. Karasu, F.; Croutxe-Barghorn, C.; Allonas, X.; Van Der Ven, L. G. J. *J. Polym. Sci. Polym. Chem.* **2014**, *52*, 3597.
13. He, M.; Chen, G.; Huang, X.; Xu, R.; Zeng, Z.; Yang, J. *Polym. Chem.* **2014**, *5*, 2951.
14. Balta, D. K.; Arsu, N.; Yagci, Y.; Jockusch, S.; Turro, N. J. *Macromolecules* **2007**, *40*, 4138.
15. Karaca, N.; Balta, D. K.; Ocal, N.; Arsu, N. *J Lumin.* **2014**, *146*, 424.
16. Tar, H.; Esen, D. S.; Aydin, M.; Ley, C.; Arsu, N.; Allonas, X. *Macromolecules.* **2013**, *46*, 3266.
17. Dong, X.; Hu, P.; Zhu, G.; Li, Z.; Liu, R.; Liu, X. *RSC Adv.* **2015**, *5*, 53342.
18. Yilmaz, G.; Acik, G.; Yagci, Y. *Macromolecules* **2012**, *45*, 2219.
19. Blake, J. A.; Gagnon, E.; Lukeman, M.; Scaiano, J. C. *Org. Lett.* **2006**, *8*, 1057.
20. Yang, J.; Xu, F.; Shi, S.; Nie, J. *Photochem. Photobiol. Sci.* **2012**, *11*, 1377.
21. Liu, S.; Shi, S.; Hou, G.; Nie, J. *Acta Odontol. Scand.* **2007**, *65*, 313.
22. Yang, J.; Shi, S.; Xu, F.; Nie, J. *Photochem. Photobiol. Sci.* **2013**, *12*, 323.
23. Esen, D. S.; Temel, G.; Balta, D. K.; Allonas, X.; Arsu, N. *Photochem. Photobiol.* **2014**, *90*, 463.
24. Aydin, M.; Arsu, N.; Yagci, Y. *Macromol. Rapid. Commun.* **2003**, *24*, 718.
25. Aydin, M.; Arsu, N.; Yagci, Y.; Jockusch, S.; Turro, N. J. *Macromolecules* **2005**, *38*, 4133.
26. Williams, A. T. R.; Winfield, S. A.; Miller, J. N. *The Analyst* **1983**, *108*, 1067.
27. Criqui, A.; Lalevée, J.; Allonas, X.; Fouassier, J. *Macromol. Chem. Phys.* **2008**, *209*, 2223.
28. Salmi, H.; Allonas, X.; Ley, C.; Defoin, A.; Ak, A. *Polym. Chem.* **2014**, *5*, 6577.
29. Lalevee, J.; Blanchard, N.; Tehfe, M. A.; Fries, C.; Morlet-Savary, F.; Gigmes, D.; Fouassier, J. P. *Polym. Chem.* **2011**, *2*, 1077.
30. Ibrahim, A.; Maurin, V.; Ley, C.; Allonas, X.; Croutxe-Barghorn, C.; Jasinski, F. *Eur. Polym. J.* **2012**, *48*, 1475.
31. Jian, Y.; He, Y.; Sun, Y.; Yang, H.; Yang, W.; Nie, J. *J. Mater. Chem. C* **2013**, *1*, 4481.
32. Arimitsu, K.; Endo, R. *Chem. Mater.* **2013**, *25*, 4461.
33. Shi, S.; Gao, H.; Wu, G.; Nie, J. *Polymer.* **2007**, *48*, 2860.
34. Shi, S.; Nie, J. *J. Biomed. Mater. Res. B* **2007**, *82B*, 44.
35. Green, W. A. Industrial Photoinitiators: A Technical guide; CRC Press Inc: Boca Raton, **2010**.
36. Melhuish, W. H. *J. Phys. Chem.* **1961**, *65*, 229.
37. Corrales, T.; Catalina, F.; Peinado, C.; Allen, N. S. *J. Photochem. Photobiol. A* **2003**, *159*, 103.
38. Tehfe, M.; Dumur, F.; Graff, B.; Morlet-Savary, F.; Gigmes, D.; Fouassier, J.; Lalevee, J. *Polym. Chem.* **2013**, *4*, 2313.
39. Bai, J.; Shi, Z. *J. Appl. Polym. Sci.* **2013**, *128*, 1785.
40. Lalevée, J.; Telitel, S.; Tehfe, M. A.; Fouassier, J. P.; Curran, D. P.; Lacôte, E. *Angew. Chem. Int. Ed.* **2012**, *51*, 5958.
41. O'Brien, A. K.; Bowman, C. N. *Macromolecules* **2006**, *39*, 2501.
42. Arsu, N.; Aydin, M.; Yagci, Y.; Jockusch, S.; Turro, N. J. Photochemistry and UV Curing: New Trends; Research Signpost: Kerala, India, **2006**.
43. Moon, S.; Kwon, Y.; Lee, J.; Choo, J. *J. Phys. Chem. A* **2001**, *105*, 3221.
44. Yamazaki, J.; Watanabe, T.; Tanaka, K. *Tetrahedron: Asymmetry* **2001**, *12*, 669.
45. Yilmaz, G.; Aydogan, B.; Temel, G.; Arsu, N.; Moszner, N.; Yagci, Y. *Macromolecules* **2010**, *43*, 4520.